Figure 2 – Supplementary Figure 1

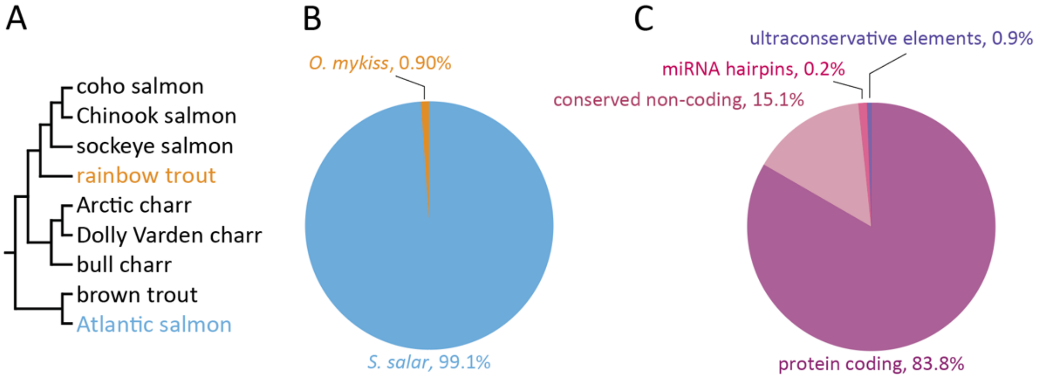

Figure 2 – Supplementary Figure 1. Design of pan-Salmoniformes targeted capture array. (A) Conserved bait sequences were derived from Atlantic salmon (*Salmo salar*) and rainbow trout (*Oncorhynchus mykiss*) reference genomes. **(B)** Relative contributions of *S. salar* and *O. mykiss* derived bait sequences to the capture array. **(C)** Classifications and relative abundances of conserved elements targeted for capture.

Figure 2 – Supplementary Figure 2

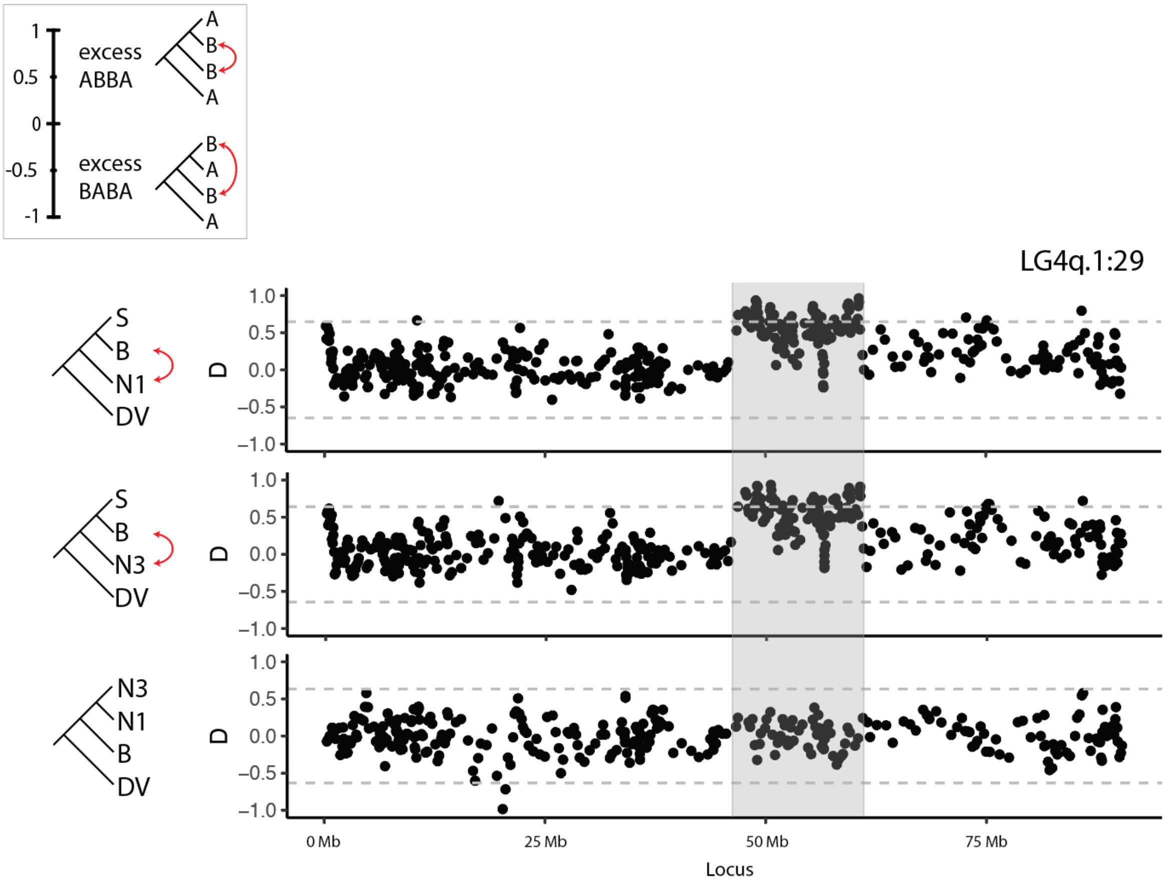

Figure 2 – Supplementary Figure 2. Sliding window plots of D showing a *large* interval of excess allele sharing. Sliding window plots for trios consisting of Smallmouth (S), Bigmouth (B), and Nosed 1 (N1), of S, B, and Nosed 3 (N3), and of N3, N1, and B. Positive D values indicate an excess of the ABBA pattern (red arrows), while negative values indicate an excess of the BABA pattern. The three plots show a common pattern of excess of allele sharing overlapping with between B and N1 and B and N3, while there is no excess of allele sharing between B and N1 over B and N3. Horizontal lines signify 3SDs from the mean.

Figure 2 – Supplementary Table 1

Morphotype	No. Individuals Pooled	No. Reads (million)	No. Reads Mapped	Median Depth	Mean Depth	"Conservome" Coverage	
						2x	10x
Bigmouth	8	72.3	35.3	66 reads	88 reads	91.6%	88.5%
Dolly Varden	3	64.1	32.4	61 reads	82 reads	91.6%	88.3%
Longhead	10	46.1	22.8	41 reads	56 reads	91.1%	85.7%
Nosed 1	5	68.8	34.9	65 reads	87 reads	91.7%	88.5%
Nosed 2	7	49.5	17.5	16 reads	20 reads	88.7%	65.5%
Nosed 3	5	68.4	34.1	63 reads	84 reads	91.6%	88.5%
Smallmouth	6	43.1	21.1	38 reads	52 reads	90.8%	84.9%
S. leucomaenis	1	55.9	25.5	50 reads	67 reads	90.5%	85.9%
White	6	36.9	18.5	34 reads	46 reads	90.6%	83.8%

Figure 2 – Supplementary Table 1. Summary of reads aligned and targeted element coverage.

Figure 2 – Supplementary Table 2

GO name	GO accession	bin size
activation of MAPK activity	GO:0000187	15
anaphase-promoting complex	GO:0005680	51
anaphase-promoting complex-dependent catabolic process	GO:0031145	41
ATP-dependent chromatin remodeling	GO:0043044	133
ATPase activity	GO:0016887	262
calcium ion binding	GO:0005509	1185
calcium, potassium:sodium antiporter activity	GO:0008273	52
carbohydrate binding	GO:0030246	111
carbohydrate metabolic process	GO:0005975	204
cell adhesion	GO:0007155	541
chemokine activity	GO:0008009	72
cullin-RING ubiquitin ligase complex	GO:0031461	23
DNA binding	GO:0003677	2972
DNA integration	GO:0015074	1571
DNA-templated transcription, initiation	GO:0006352	36
ferric iron binding	GO:0008199	24
fructose-bisphosphate aldolase activity	GO:0004332	27
hexose metabolic process	GO:0019318	34
homophilic cell adhesion via plasma membrane adhesion molecules	GO:0007156	362
iron ion transport	GO:0006826	23
isomerase activity	GO:0016853	45
MAP kinase activity	GO:0004707	52
nucleic acid binding	GO:0003676	2731
oligopeptide transport	GO:0006857	20
phosphatidylinositol metabolic process	GO:0046488	49
phosphatidylinositol phosphate kinase activity	GO:0016307	47
receptor tyrosine kinase binding	GO:0030971	28
regulation of mitotic metaphase/anaphase transition	GO:0030071	44
sensory perception of sound	GO:0007605	69
skeletal muscle fiber development	GO:0048741	44
SWI/SNF complex	GO:0016514	147
transcription coactivator activity	GO:0003713	164
transcription factor TFIID complex	GO:0005669	38
transmembrane transport	GO:0055085	1148
transmembrane transporter activity	GO:0022857	306
transporter activity	GO:0005215	218
transposition, DNA-mediated	GO:0006313	1551
ubiquitin protein ligase binding	GO:0031625	28
vesicle-mediated transport	GO:0016192	250

Figure 2 – Supplementary Table 2. Table of significantly underrepresented GO terms. This table contains the set of significantly underrepresented GO terms among all sample libraries (Benjamini-Hochberg FDR < 0.05).

Figure 2 – Supplementary Table 3

Pop 1	Pop 2	Pop 3	D_{tree} (%)	$ƒ_4$-ratio (%)	p-value	Z-score
S	N3	W	3.9	8.6	0	13.0*
S	N1	W	3.7	8.2	0	11.4*
S	N3	L	2.8	6.3	0	11.4*
S	N1	L	2.2	4.9	1.18E-16	8.3*
S	B	N1	4.2	9.0	1.56E-15	8.0*
S	B	W	2.2	4.7	1.26E-14	7.7*
B	N3	W	1.8	4.1	2.44E-14	7.6*
L	W	N1	2.2	4.5	2.73E-13	7.3*
L	W	B	1.7	3.9	2.76E-13	7.3*
B	N1	W	1.7	3.7	2.11E-12	7.0*
S	B	N3	3.6	8.3	2.31E-11	6.7*
L	W	N3	1.8	3.8	4.65E-09	5.9*
B	N3	L	1.8	4.0	6.52E-07	5.0*
S	B	L	1.1	2.4	1.01E-04	3.9*
B	N1	L	1.2	2.6	3.59E-04	3.6*
N1	N3	L	0.7	1.5	1.13E-03	3.3*
L	W	S	0.5	1.4	2.86E-03	3.0
N1	N3	S	0.4	0.9	5.72E-02	1.9
N1	N3	W	0.2	0.5	2.79E-01	1.1
N3	N1	B	0.3	0.7	2.86E-01	1.1

Figure 2 – Supplementary Table 3. Table of D_{tree} scores, $ƒ_4$-admixture ratios, and Z-scores for each of the 20 trios contained within the Lake Kronotskoe species flock. 16 trios were found to have a significant, though minimal, contribution of introgressed alleles (asterisks)(Holm-Bonferoni, FWER < 0.01). B, Bigmouth; L, Longhead; N1, Nosed 1; N3, Nosed 3; S, Smallmouth; W, White.

Figure 7 – Supplementary Figure 1

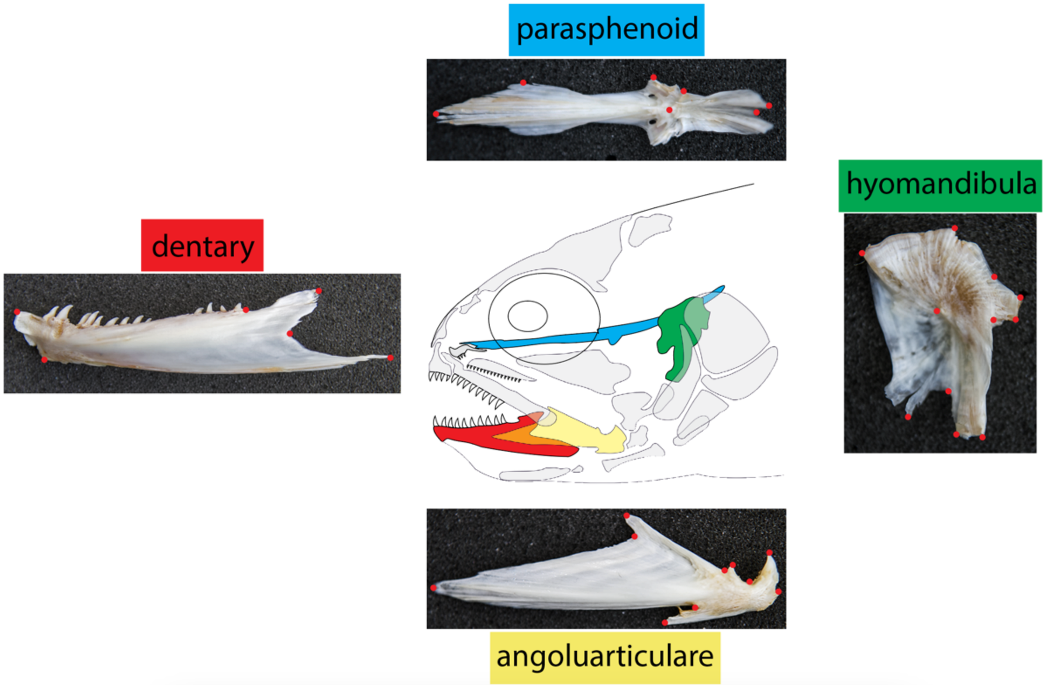

Figure 7 – Supplementary Figure 1. Landmarks used to geomorphic morphometric analyses. Landmarks were assigned to each of four bones. The dentary (red), the parasphenoid (blue), the hyomandibula (green), and the anguloarticulare (yellow).

Figure 7 – Supplementary Figure 2 Figure 7 – Supplementary Figure 2

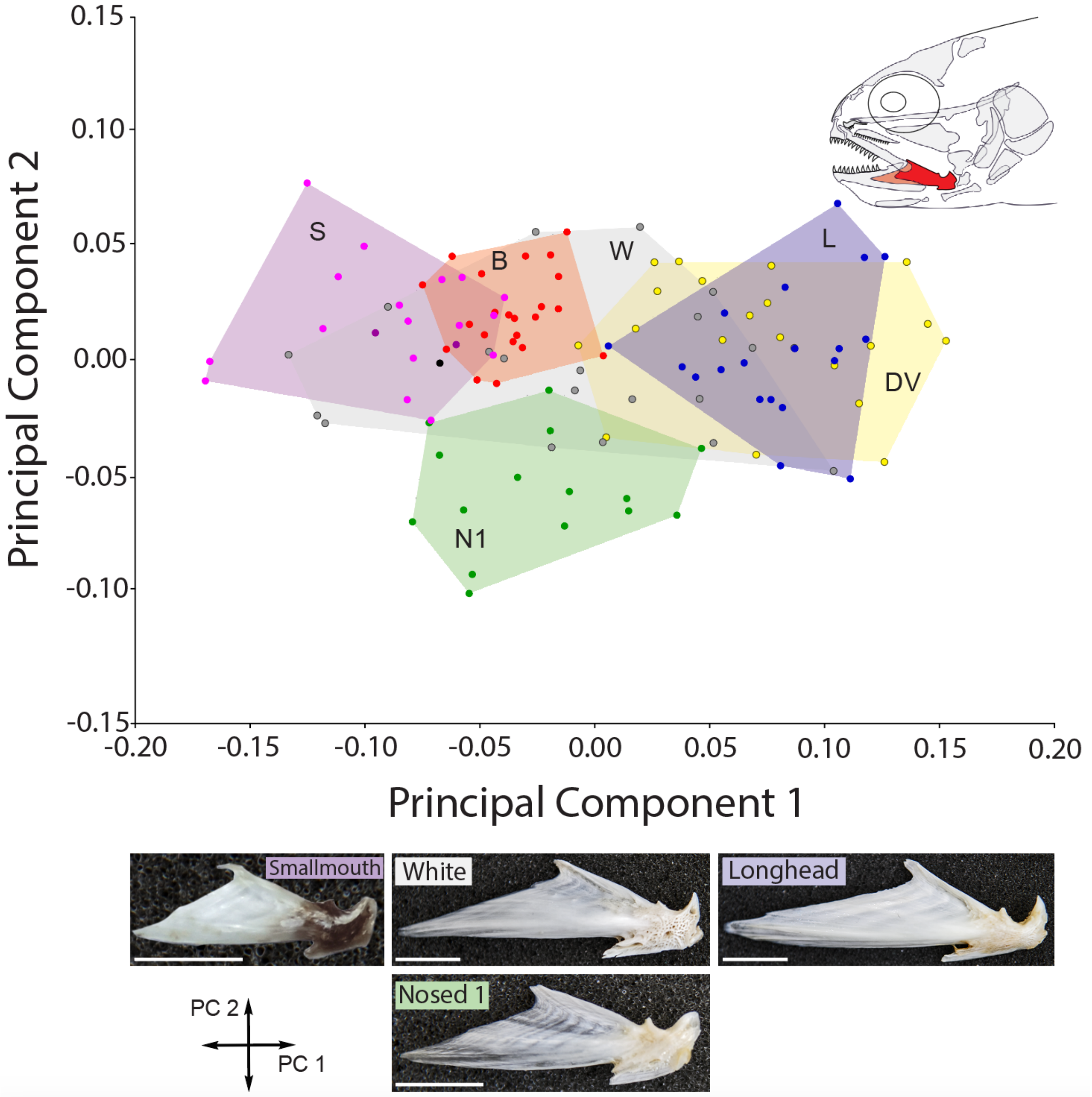

Figure 7 – Supplementary Figure 2. Geometric morphometric analyses of anguloarticulare among Lake Kronotskoe morphs. Procrustes analyses identified highly significant differences in shape (Procrustes ANOVA $F_{80;1760}$=18.88 p<0.0001). Scale bar = 10mm.

Figure 7 – Supplementary Figure 3

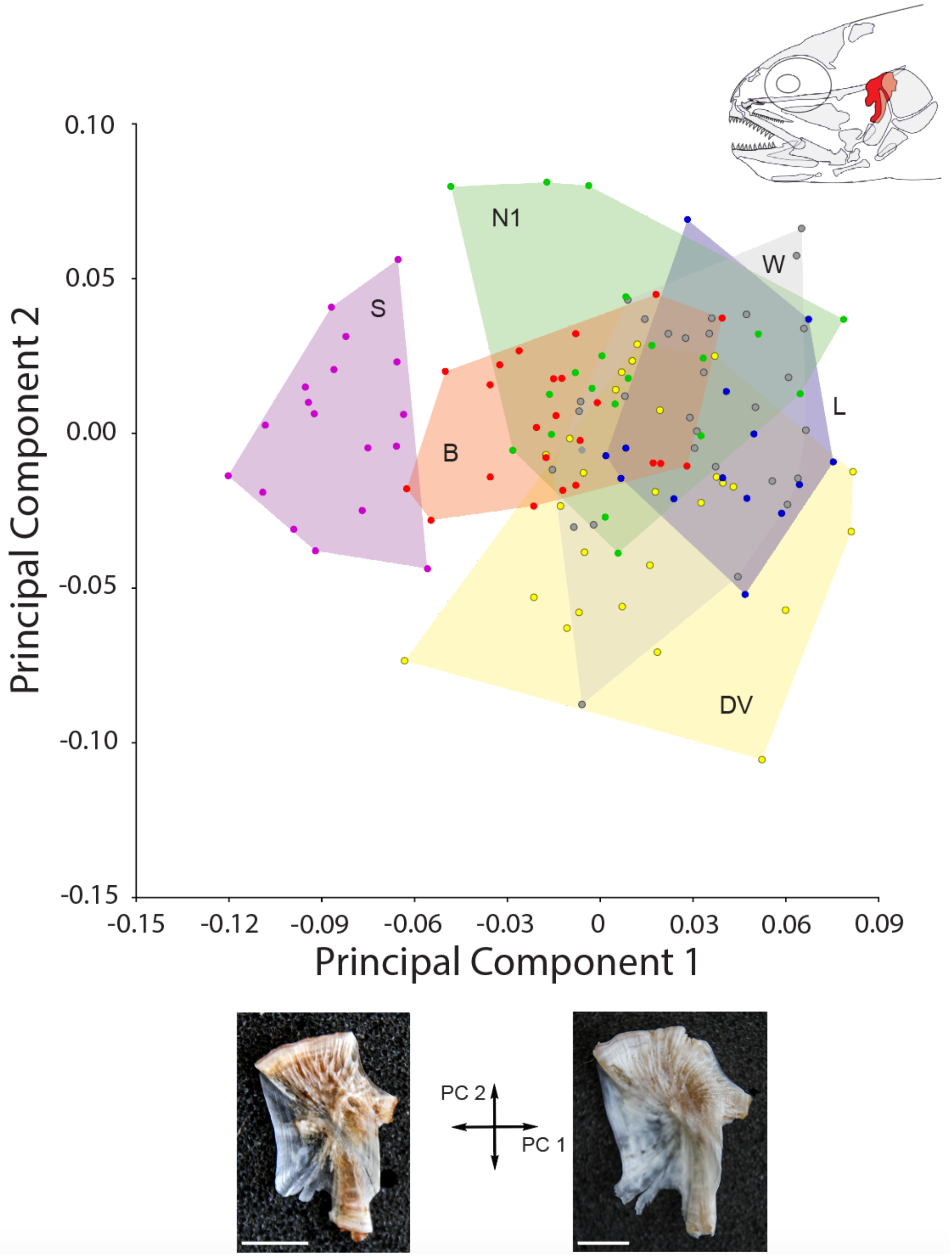

Figure 7 – Supplementary Figure 3. Geometric morphometric analyses of hyomandibula among Lake Kronotskoe morphs. Procrustes analyses identified significant differences in shape (Procrustes ANOVA $F_{60;1212}$=6.55 p<0.001) with Smallmouth morphs possessing the most distinct shape.

Figure 7 – Supplementary Figure 4

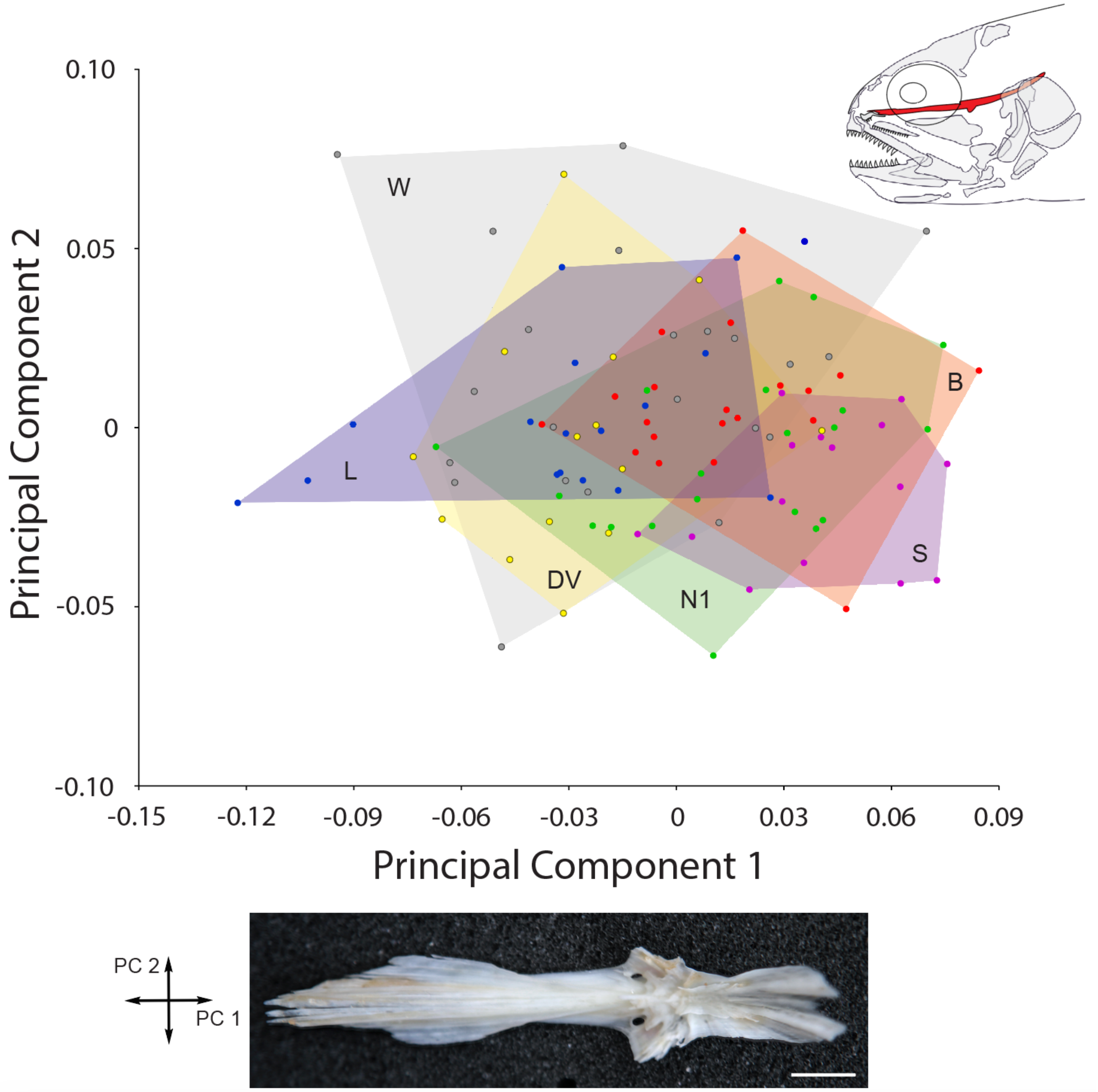

Figure 7 – Supplementary Figure 4. Geometric morphometric analyses of parasphenoid among Lake Kronotskoe morphs. Procrustes analyses identified no significant differences in shape. Scale bar = 10mm.